

# **Supporting Information:**

## **Tetrel, Nonconventional Hydrogen Bonds, and Noticeable Role of Dispersion in Complexes of Fluoroform and Carbon Dichalcogenides**

Thanh-Nam Huynh,<sup>†</sup> Nguyen Thi Minh Nguyet,<sup>‡</sup> Bui Duc Ai,<sup>‡</sup> and Nguyen Tien  
Trung<sup>\*,‡,¶</sup>

*†Institute of Catalysis Research and Technology, Karlsruhe Institute of Technology,  
Hermann-von-Helmholtz-Platz 1, 76344 Eggenstein-Leopoldshafen, Germany*

*‡Laboratory of Computational Chemistry and Modelling (LCCM), Quy Nhon University,  
170 An Duong Vuong Street, Quy Nhon City 590000, Vietnam.*

*¶Faculty of Natural Sciences, Quy Nhon University, 170 An Duong Vuong Street, Quy  
Nhon City 590000, Vietnam*

E-mail: [nguyentientrung@qnu.edu.vn](mailto:nguyentientrung@qnu.edu.vn)

# Contents

<b>S1 Noncovalent Interaction Conformational Sampling</b>	<b>S-3</b>
<b>S2 Complex Stability</b>	<b>S-7</b>
<b>S3 NBO analyses</b>	<b>S-8</b>
<b>S4 Monomer Properties</b>	<b>S-10</b>
<b>S5 Atoms-In-Molecules Analyses</b>	<b>S-11</b>
<b>S6 Interaction Energy and Contributions via SAPT Analysis</b>	<b>S-13</b>
<b>References</b>	<b>S-16</b>

## S1 Noncovalent Interaction Conformational Sampling

As mentioned in the main text, we employed a noncovalent interaction conformational search using the CREST workflow<sup>S1</sup> at the semi-empirical GFN2-xTB theory level<sup>S2</sup> to screen all the possible geometrical configurations of the studied complexes within a window of 3 kcal mol<sup>-1</sup>. Figure S1-S8 depict the geometries of the most stable structures for each complex and Table S1 tabulates the respective electronic energy relative to their most stable structure between them predicted at the GFN2-xTB (within the CREST workflow), MP2, and CCSD(T) levels.

Remarkably, almost all geometries of the stable complexes were included in the ensembles generated by the workflows. In addition, relative stability of the most stable oxygen-containing complexes, as predicted by the CCSD(T) method, were accurately reproduced at the GFN2-xTB level. For the oxygen-free systems, however, stability predictions showed inconsistencies between the semi-empirical and high-level methods. It is worth noting that the trends in stability were not consistently aligned even between the MP2 and CCSD(T) levels for these complexes.

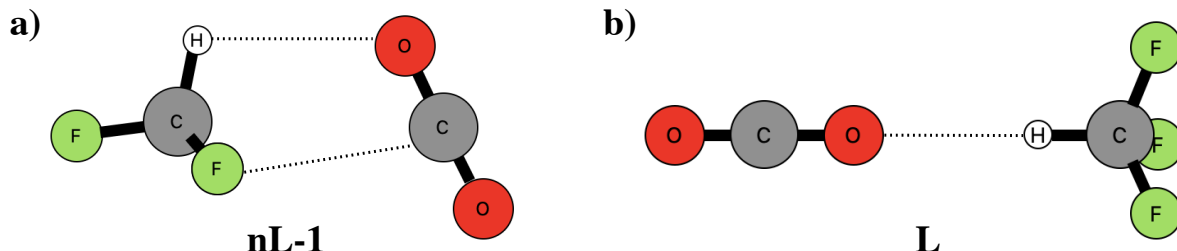


Figure S1: Geometries of the more stable structures for the  $\text{F}_3\text{CH}\cdots\text{OCO}$  complex.

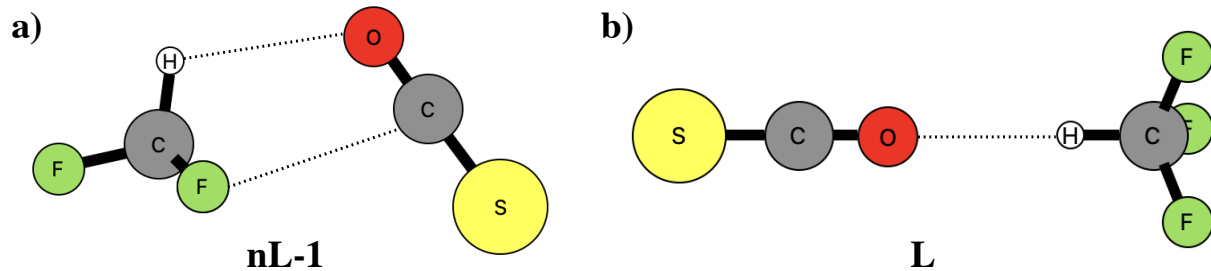


Figure S2: Geometries of the more stable structures for the  $\text{F}_3\text{CH}\cdots\text{OCS}$  complex.

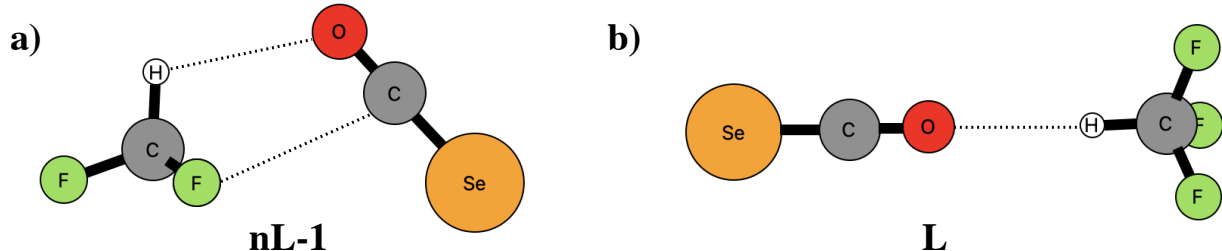


Figure S3: Geometries of the more stable structures for the  $\text{F}_3\text{CH}\cdots\text{OCSe}$  complex.

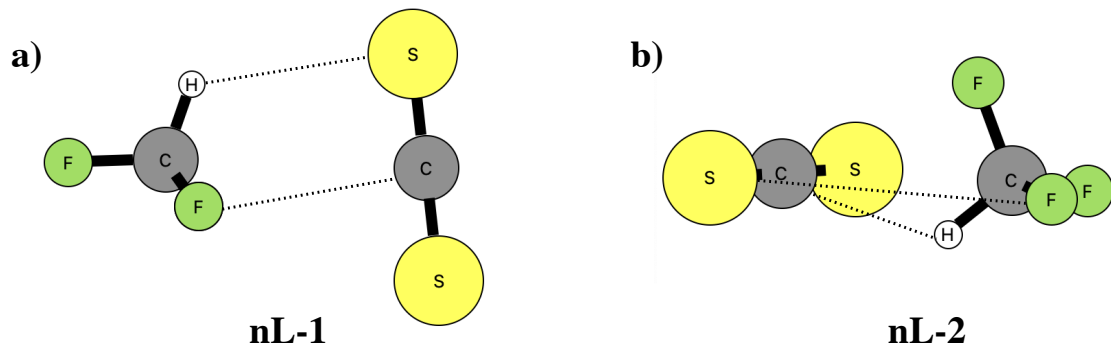


Figure S4: Geometries of the more stable structures for the  $\text{F}_3\text{CH}\cdots\text{SCS}$  complex.

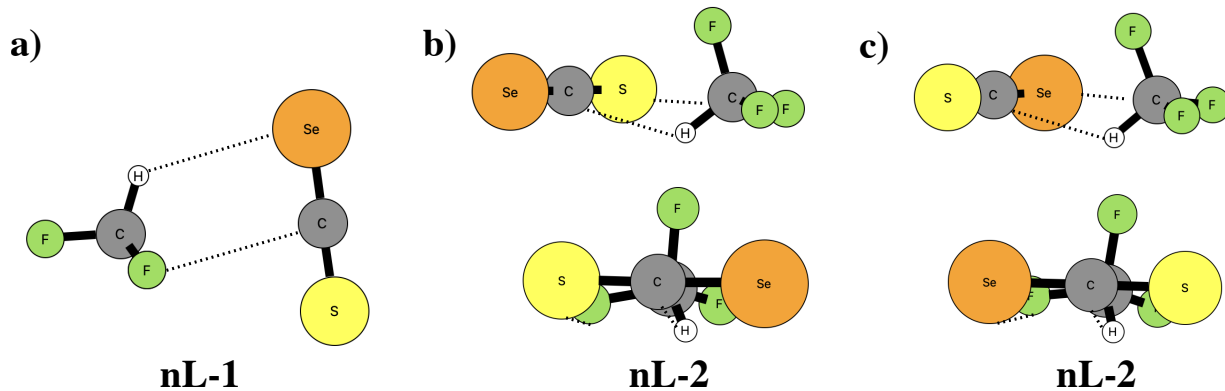


Figure S5: Geometries of the more stable structures for the  $\text{F}_3\text{CH}\cdots\text{SCSe}$  complex.

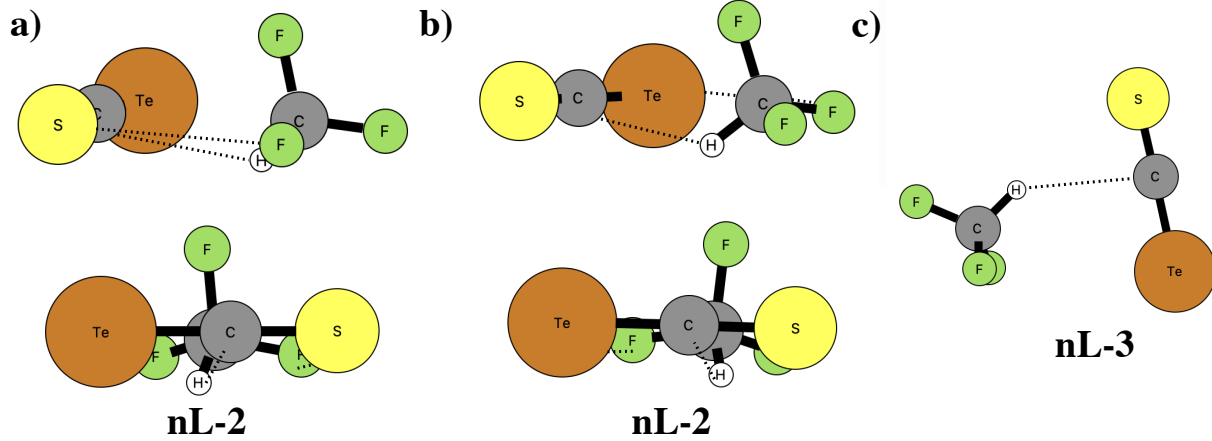


Figure S6: Geometries of the more stable structures for the  $\text{F}_3\text{CH}\cdots\text{SCTe}$  complex.

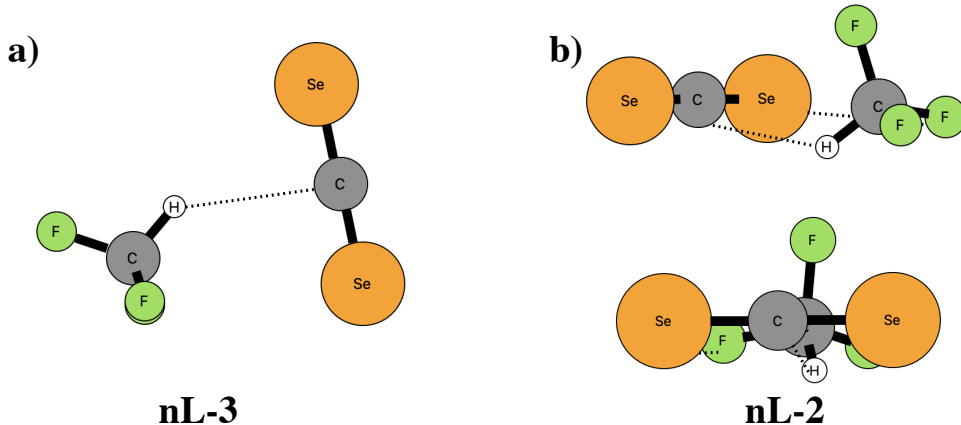


Figure S7: Geometries of the more stable structures for the  $\text{F}_3\text{CH}\cdots\text{SeCSe}$  complex.

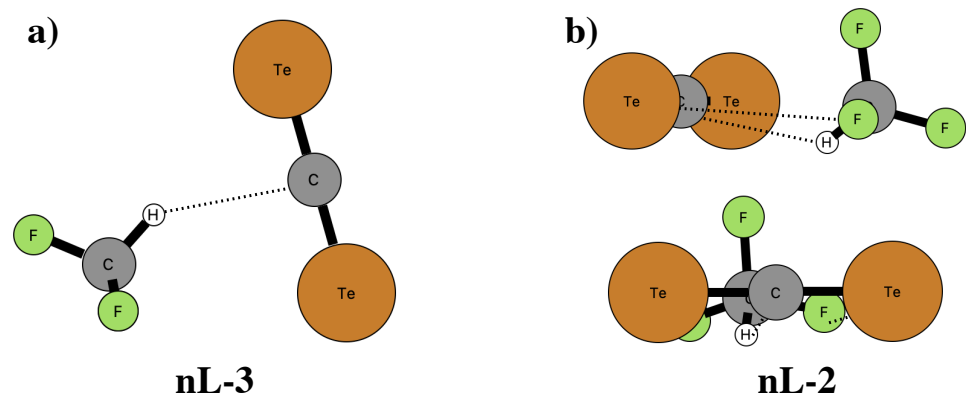


Figure S8: Geometries of the more stable structures for the  $\text{F}_3\text{CH}\cdots\text{TeCTe}$  complex.

Table S1: Relative electronic energy with respect to the most stable structures of the  $\text{F}_3\text{CH}\cdots\text{XOY}$  ( $\text{X} = \text{O}, \text{S}, \text{Se}, \text{Te}$ ) complexes predicted by different methods. The corresponding structures are depicted in Figure S1-S8. Structures **a** correspond to the structures with lowest interaction energies (not necessarily corresponding to the lowest-lying structures).

Complex	Structure	GFN2-xTB	MP2	CC
$\text{F}_3\text{CH}\cdots\text{OCO}$	a	0	0	0
	b	0.7	2.7	2.9
$\text{F}_3\text{CH}\cdots\text{OCS}$	a	0	0	0
	b	1.5	2.8	2.5
$\text{F}_3\text{CH}\cdots\text{OCSe}$	a	0	0	0
	b	2.8	2.6	2.5
$\text{F}_3\text{CH}\cdots\text{SCS}$	a	3.2*	0	0
	b	0	0.2	0
$\text{F}_3\text{CH}\cdots\text{SCSe}$	a	3.4	0.7	0.1
	b	1.2	0	0
	c	0	0.2	0.3
$\text{F}_3\text{CH}\cdots\text{SCTe}$	a	12.3*	0.1	0
	b	2.6*	0	0.3
	c	0	0.5	1.0
$\text{F}_3\text{CH}\cdots\text{SeCSe}$	a	1.1	0	0
	b	0	0.5	0.3
$\text{F}_3\text{CH}\cdots\text{TeCTe}$	a	0.2	0.3	0.1
	b	0	0	0

\* MP2 geometry was considerably different from the initial GFN2-xTB geometry.

## S2 Complex Stability

Table S2: Comparison on interaction energies in  $\text{kJ mol}^{-1}$  of hydrogen bonding complexes predicted by the CCSD(T)/6-311++G(3df,2pd)//MP2/6-311++G(3df,2pd) and MP2/6-311++G(3df,2pd) levels. The differences in interaction energies between the two methods are given in  $\Delta\Delta E_b^*$ , defined as  $\Delta\Delta E_b^* = \Delta E_b^{\text{CC},*} - \Delta E_b^{\text{MP2},*}$ .

Complex	$\Delta E_b^{\text{MP2}}$	$\Delta E_b^{\text{MP2},*}$	$\Delta E_b^{\text{CC}}$	$\Delta E_b^{\text{CC},*}$	$\Delta\Delta E_b^*$
$\text{F}_3\text{CH}\cdots\text{OCO(L)}$	-5.6	-3.7	-6.1	-4.1	-0.4
$\text{F}_3\text{CH}\cdots\text{OCO(nL)}$	-8.0	-4.8	-8.7	-5.2	-0.4
$\text{F}_3\text{CH}\cdots\text{OCS(L)}$	-6.3	-4.1	-6.7	-4.4	-0.3
$\text{F}_3\text{CH}\cdots\text{OCS(nL)}$	-8.8	-5.1	-9.0	-5.1	0.0
$\text{F}_3\text{CH}\cdots\text{OCSe(L)}$	-5.9	-3.9	-6.1	-4.0	-0.1
$\text{F}_3\text{CH}\cdots\text{OCSe(nL)}$	-8.4	-4.9	-8.4	-4.6	0.2
$\text{F}_3\text{CH}\cdots\text{SCS(nL)}$	-8.5	-4.5	-7.6	-3.3	1.4
$\text{F}_3\text{CH}\cdots\text{SCSe(nL)}$	-8.8	-5.1	-8.1	-3.9	1.5
$\text{F}_3\text{CH}\cdots\text{SCTe(nL)}$	-9.7	-4.5	-7.9	-2.6	1.9
$\text{F}_3\text{CH}\cdots\text{SeCSe(nL)}$	-9.5	-6.2	-8.1	-4.6	1.6
$\text{F}_3\text{CH}\cdots\text{TeCTe(nL)}$	-14.6	-8.5	-11.8	-5.8	2.7

### S3 NBO analyses

Table S3: Delocalization characteristics of  $\text{F}_3\text{CH}\cdots\text{OCY}$  complexes ( $\text{Y} = \text{O}, \text{S}, \text{Se}$ ) derived from NBO 6.0 calculations.

Complex	Delocalization	$E^{(2)}$ (kJ mol $^{-1}$ )
CHF3-OCO( <b>L</b> )	$n(\text{O7}) \rightarrow \sigma^*(\text{C1-H2})$	5.40
	$\sigma(\text{C6-O7}) \rightarrow \sigma^*(\text{C1-H2})$	0.25
	$\sigma(\text{C6-O8}) \rightarrow \sigma^*(\text{C1-H2})$	0.25
	$\sigma(\text{C1-H2}) \rightarrow \sigma^*(\text{C6-O7})$	1.00
CHF3-OCS( <b>L</b> )	$n(\text{O7}) \rightarrow \sigma^*(\text{C1-H2})$	5.19
	$n(\text{S8}) \rightarrow \sigma^*(\text{C1-H2})$	0.21
	$\sigma(\text{C6-O7}) \rightarrow \sigma^*(\text{C1-H2})$	0.21
	$\sigma(\text{C6-S8}) \rightarrow \sigma^*(\text{C1-H2})$	0.59
	$\sigma(\text{C1-H2}) \rightarrow \sigma^*(\text{C6-O7})$	1.00
CHF3-OCSe( <b>L</b> )	$n(\text{O7}) \rightarrow \sigma^*(\text{C1-H2})$	4.69
	$n(\text{Se8}) \rightarrow \sigma^*(\text{C1-H2})$	0.21
	$\sigma(\text{C6-Se8}) \rightarrow \sigma^*(\text{C1-H2})$	0.63
	$\sigma(\text{C1-H2}) \rightarrow \sigma^*(\text{C6-O7})$	1.09
CHF3-OCO( <b>nL-1</b> )	$n(\text{O7}) \rightarrow \sigma^*(\text{C1-H2})$	0.42
	$n(\text{O7}) \rightarrow \sigma^*(\text{C1-F3})$	1.00
	$n(\text{O7}) \rightarrow \sigma^*(\text{C1-F4})$	0.29
	$n(\text{O7}) \rightarrow \sigma^*(\text{C1-F5})$	0.29
	$n(\text{F4}) \rightarrow \pi^*(\text{C6-O8})$	0.71
	$n(\text{F5}) \rightarrow \pi^*(\text{C6-O8})$	0.71
CHF3-OCS( <b>nL-1</b> )	$n(\text{O7}) \rightarrow \sigma^*(\text{C1-H2})$	0.50
	$n(\text{O7}) \rightarrow \sigma^*(\text{C1-F3})$	0.84
	$n(\text{F4}) \rightarrow \pi^*(\text{C6-S8})$	0.33
	$n(\text{F4}) \rightarrow \pi^*(\text{C6-S8})$	0.92
	$n(\text{F5}) \rightarrow \pi^*(\text{C6-S8})$	0.33
	$n(\text{F5}) \rightarrow \pi^*(\text{C6-S8})$	0.92
	$\sigma(\text{C1-H2}) \rightarrow \sigma^*(\text{C6-O7})$	0.33
CHF3-OCSe( <b>nL-1</b> )	$n(\text{O7}) \rightarrow \sigma^*(\text{C1-H2})$	0.50
	$\pi(\text{C6-O7}) \rightarrow \sigma^*(\text{C1-F3})$	0.63
	$n(\text{F4}) \rightarrow \pi^*(\text{C6-O7})$	0.46
	$n(\text{F4}) \rightarrow \pi^*(\text{C6-O7})$	0.75
	$n(\text{F5}) \rightarrow \pi^*(\text{C6-O7})$	0.46
	$n(\text{F5}) \rightarrow \pi^*(\text{C6-O7})$	0.75
	$\sigma(\text{C1-H2}) \rightarrow \sigma^*(\text{C6-O7})$	0.42
	$\sigma(\text{C1-H2}) \rightarrow \sigma^*(\text{C6-Se8})$	0.25

Table S4: Delocalization characteristics of  $\text{F}_3\text{CH}\cdots\text{XCY}$  complexes ( $\text{X}, \text{Y} = \text{S}, \text{Se}, \text{Te}$ ) derived from NBO 6.0 calculations.

Complex	Delocalization	$E^{(2)}$ (kJ mol $^{-1}$ )
CHF <sub>3</sub> -SCS( <b>nL-1</b> )	$\text{n}(\text{S8}) \rightarrow \sigma^*(\text{C1-H2})$	0.79
	$\text{n}(\text{S8}) \rightarrow \sigma^*(\text{C1-H2})$	3.05
	$\text{n}(\text{S8}) \rightarrow \sigma^*(\text{C1-F5})$	0.59
	$\text{n}(\text{F3}) \rightarrow \pi^*(\text{C6-S7})$	0.38
	$\text{n}(\text{F3}) \rightarrow \pi^*(\text{C6-S7})$	0.33
	$\text{n}(\text{F4}) \rightarrow \pi^*(\text{C6-S7})$	0.38
	$\text{n}(\text{F4}) \rightarrow \pi^*(\text{C6-S7})$	0.33
	$\sigma(\text{C1-H2}) \rightarrow \pi^*(\text{C6-S7})$	0.21
CHF <sub>3</sub> -SCSe( <b>nL-1</b> )	$\text{n}(\text{Se8}) \rightarrow \sigma^*(\text{C1-H2})$	0.75
	$\text{n}(\text{Se8}) \rightarrow \sigma^*(\text{C1-H2})$	4.39
	$\text{n}(\text{Se8}) \rightarrow \sigma^*(\text{C1-F4})$	0.42
	$\text{n}(\text{F3}) \rightarrow \pi^*(\text{C6-S7})$	0.33
	$\text{n}(\text{F5}) \rightarrow \pi^*(\text{C6-S7})$	0.33
	$\sigma(\text{C1-H2}) \rightarrow \pi^*(\text{C6-S7})$	0.38
CHF <sub>3</sub> -SCTe( <b>nL-2</b> )	$\text{n}(\text{Te8}) \rightarrow \sigma^*(\text{C1-H2})$	0.46
	$\text{n}(\text{Te8}) \rightarrow \sigma^*(\text{C1-H2})$	1.30
	$\text{n}(\text{Te8}) \rightarrow \sigma^*(\text{C1-F4})$	0.25
	$\pi(\text{C6-S7}) \rightarrow \sigma^*(\text{C1-F4})$	0.54
	$\sigma(\text{C6-Te8}) \rightarrow \sigma^*(\text{C1-H2})$	0.29
	$\text{n}(\text{F3}) \rightarrow \pi^*(\text{C6-S7})$	0.38
	$\text{n}(\text{F3}) \rightarrow \sigma^*(\text{C6-S7})$	0.25
	$\text{n}(\text{F3}) \rightarrow \pi^*(\text{C6-S7})$	0.42
	$\sigma(\text{C1-H2}) \rightarrow \pi^*(\text{C6-S7})$	2.51
	$\sigma(\text{C1-H2}) \rightarrow \sigma^*(\text{C6-Te8})$	0.25
CHF <sub>3</sub> -SeCSe( <b>nL-3</b> )	$\text{n}(\text{Se7}) \rightarrow \sigma^*(\text{C1-H2})$	0.42
	$\text{n}(\text{Se7}) \rightarrow \sigma^*(\text{C1-H2})$	2.38
	$\text{n}(\text{Se8}) \rightarrow \sigma^*(\text{C1-H2})$	0.25
	$\pi(\text{C6-Se8}) \rightarrow \sigma^*(\text{C1-F5})$	0.46
	$\sigma(\text{C6-Se8}) \rightarrow \sigma^*(\text{C1-H2})$	0.50
	$\sigma(\text{C1-H2}) \rightarrow \pi^*(\text{C6-Se8})$	2.51
CHF <sub>3</sub> -TeCTe( <b>nL-3</b> )	$\text{n}(\text{Te7}) \rightarrow \sigma^*(\text{C1-H2})$	0.59
	$\text{n}(\text{Te7}) \rightarrow \sigma^*(\text{C1-H2})$	3.64
	$\text{n}(\text{Te8}) \rightarrow \sigma^*(\text{C1-H2})$	0.29
	$\pi(\text{C6-Te8}) \rightarrow \sigma^*(\text{C1-H2})$	0.46
	$\pi(\text{C6-Te8}) \rightarrow \sigma^*(\text{C1-F3})$	0.79
	$\sigma(\text{C6-Te8}) \rightarrow \sigma^*(\text{C1-H2})$	0.63
	$\sigma(\text{C1-H2}) \rightarrow \pi^*(\text{C6-Te8})$	3.64

## S4 Monomer Properties

Table S5: Proton Affinity of OCY molecules (Y = O, S, Se) calculated at CCSD(T)/6-311++G(3df,2pd)//MP2/6-311++G(3df,2pd).

Molecule	Proton Affinity (kJ mol <sup>-1</sup> )
OCO	493
OCS	556
OCSe	562

## S5 Atoms-In-Molecules Analyses

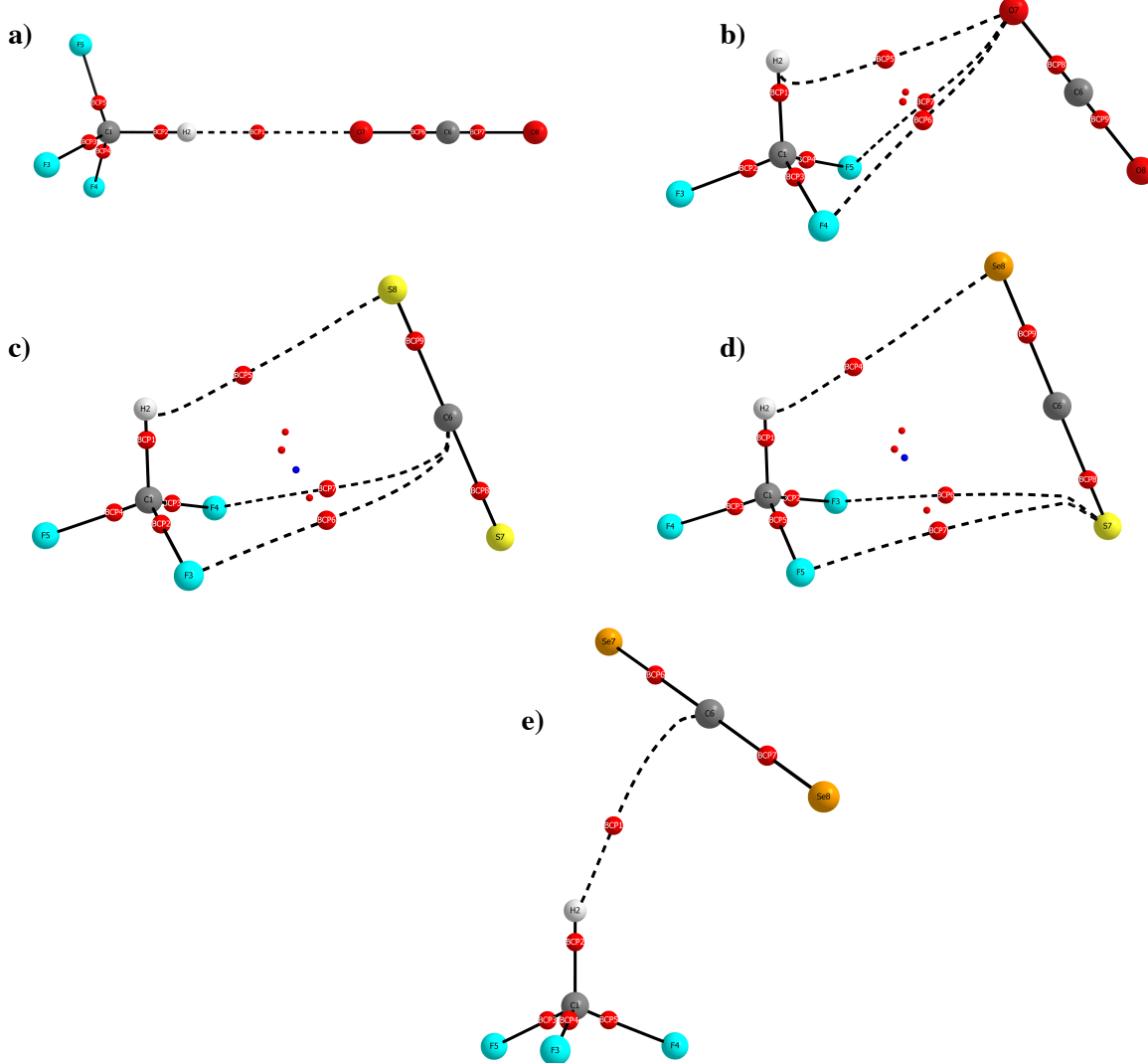


Figure S9: Representative electron density topology for the studied complexes obtained from AIM analyses.

Table S6: Selected parameters at BCPs of nonconventional hydrogen bonded interactions in linear  $\text{F}_3\text{CH}\cdots\text{OCX}$  complexes (X: O, S, Se) (density at MP2/6-311++G(3df,2pd)).

Compound	Interaction Type	Atoms	$\rho(r)$ ( $\times 10^3$ a.u.)	$\nabla^2 \rho(r)$ (a.u.)	$H(r)$ (a.u.)	$\frac{-G(r)}{V(r)}$	$E_{\text{HB}}$ (kJ mol $^{-1}$ )
CHF3-OCO(L)	C-H $\cdots$ O	H2-O7	8.4	0.035	0.0015	1.27	-7.4
CHF3-OCS(L)	C-H $\cdots$ O	H2-O7	8.8	0.036	0.0015	1.26	-7.8
CHF3-OCSe(L)	C-H $\cdots$ O	H2-O7	8.5	0.035	0.0015	1.26	-7.5

Table S7: Selected parameters at BCPs of nonconventional hydrogen bonded interactions in linear  $\text{F}_3\text{CH}\cdots\text{OCX}$  complexes (X: O, S, Se) (density at CCSD(T)/6-311++G(3df,2pd)//MP2/6-311++G(3df,2pd)).

Compound	Interaction Type	Atoms	$\rho(r)$ ( $\times 10^3$ a.u.)	$\nabla^2 \rho(r)$ (a.u.)	$H(r)$ (a.u.)	$\frac{-G(r)}{V(r)}$	$E_{\text{HB}}$ (kJ mol $^{-1}$ )
CHF3-OCO(L)	C-H $\cdots$ O	H2-O7	7.8	0.036	0.0017	1.32	-7.1
CHF3-OCS(L)	C-H $\cdots$ O	H2-O7	8.1	0.037	0.0018	1.31	-7.5
CHF3-OCSe(L)	C-H $\cdots$ O	H2-O7	7.8	0.036	0.0017	1.31	-7.1

Table S8: Selected parameters at BCPs of nonconventional hydrogen bonded interactions in non-linear  $\text{F}_3\text{CH}\cdots\text{OCY}$  complexes (Y= O, S, Se) (density at MP2/6-311++G(3df,2pd)).

Compound	Interaction Type	Atoms	$\rho(r)$ ( $\times 10^3$ a.u.)	$\nabla^2 \rho(r)$ (a.u.)	$H(r)$ (a.u.)	$\frac{-G(r)}{V(r)}$	$E_{\text{HB}}$ (kJ mol $^{-1}$ )
CHF3-OCO( <b>nL-1</b> )	C-H $\cdots$ O	H2-O7	6.7	0.028	0.0012	1.27	-6.0
	C-F $\cdots$ O	F4-O7	6.1	0.027	0.0010	1.21	-
	C-F $\cdots$ O	F5-O7	6.1	0.027	0.0010	1.21	-
CHF3-OCS( <b>nL-1</b> )	C-H $\cdots$ O	H2-O7	7.1	0.028	0.0012	1.24	-6.2
	C-F $\cdots$ O	F4-O7	5.7	0.026	0.0011	1.24	-
	C-F $\cdots$ O	F5-O7	5.7	0.026	0.0011	1.24	-
CHF3-OCSe( <b>nL-1</b> )	C-H $\cdots$ O	H2-O7	7.0	0.028	0.0012	1.25	-7.5
	C-F $\cdots$ O	F4-O7	5.5	0.026	0.0011	1.26	-
	C-F $\cdots$ O	F4-O7	5.5	0.026	0.0011	1.26	-

Table S9: Selected parameters at BCPs of nonconventional hydrogen bonded interactions in non-linear  $\text{F}_3\text{CH}\cdots\text{XCY}$  complexes ( $\text{X}, \text{Y} = \text{S}, \text{Se}, \text{Te}$ ) (density at MP2/6-311++G(3df,2pd)).

Compound	Interaction Type	Atoms	$\rho(r)$ ( $\times 10^3$ a.u.)	$\nabla^2\rho(r)$ (a.u.)	$H(r)$ (a.u.)	$\frac{-G(r)}{V(r)}$	$E_{\text{HB}}$ (kJ mol $^{-1}$ )
CHF <sub>3</sub> -SCS( <b>nL-1</b> )	C-H $\cdots$ S	H2-S7	5.8	0.018	0.0008	1.29	-3.7
	C-F $\cdots$ C	F4-C7	4.1	0.017	0.0009	1.36	-
	C-F $\cdots$ C	F5-C7	4.1	0.017	0.0009	1.36	-
CHF <sub>3</sub> -SCSe( <b>nL-1</b> )	C-H $\cdots$ Se	H2-Se7 <sup>a</sup>	5.5	0.016	0.0007	1.28	-3.3
	C-F $\cdots$ C	F3-S7 <sup>b</sup>	4.1	0.017	0.0008	1.34	-
	C-F $\cdots$ C	F5-S7 <sup>b</sup>	4.1	0.017	0.0008	1.34	-
CHF <sub>3</sub> -SCTe( <b>nL-2</b> )	C-H $\cdots$ C	H2-C6	6.7	0.022	0.0009	1.26	-4.7
CHF <sub>3</sub> -SeCSe( <b>nL-3</b> )	C-H $\cdots$ C	H2-C6	6.5	0.021	0.0009	1.29	-4.3
CHF <sub>3</sub> -TeCTe( <b>nL-3</b> )	C-H $\cdots$ C	H2-C6	7.9	0.024	0.0009	1.23	-5.4

<sup>a</sup> The BCP should connect H and the electrostatically negative region between C-Se bond.

<sup>b</sup> The BCP should connect F and C atoms.

## S6 Interaction Energy and Contributions via SAPT Analysis

The SAPT analysis has been widely applied to describing the strength and nature of non-covalent interactions. Figure S10 demonstrates the excellent capability of different high-order SAPT methods for very weak interactions in the nonlinear complexes as they are able to reproduce the small interaction energies and preserve their general trend. In general, the SAPT methods underestimate the interaction energy of all investigated complexes, as compared to  $\Delta E_b^{\text{CC}*}$ , calculated via Eq. 3. The variants with MP2 correction ( $\delta\text{MP2}$ ) improve estimations by an average amount of  $0.8 \text{ kJ mol}^{-1}$ , but still give at best an MAE of  $2.6 \text{ kJ mol}^{-1}$  (SAPT2+(3) $\delta\text{MP2}$ ). This difference here, however, is easily explained from the reference perspective as the supramolecular approach accounts for monomers' relaxation, while the SAPT methods concern interactions between non-relaxed monomers in a given optimized dimers' configuration. Arguably, the SAPT's interaction energies can be considered better at describing the noncovalent interactions than its supramolecular counterpart.<sup>S3</sup> Regardless, it is generally reliable to use the interaction energies and the decomposed energy terms to further investigate the nature of noncovalent interactions of interest.

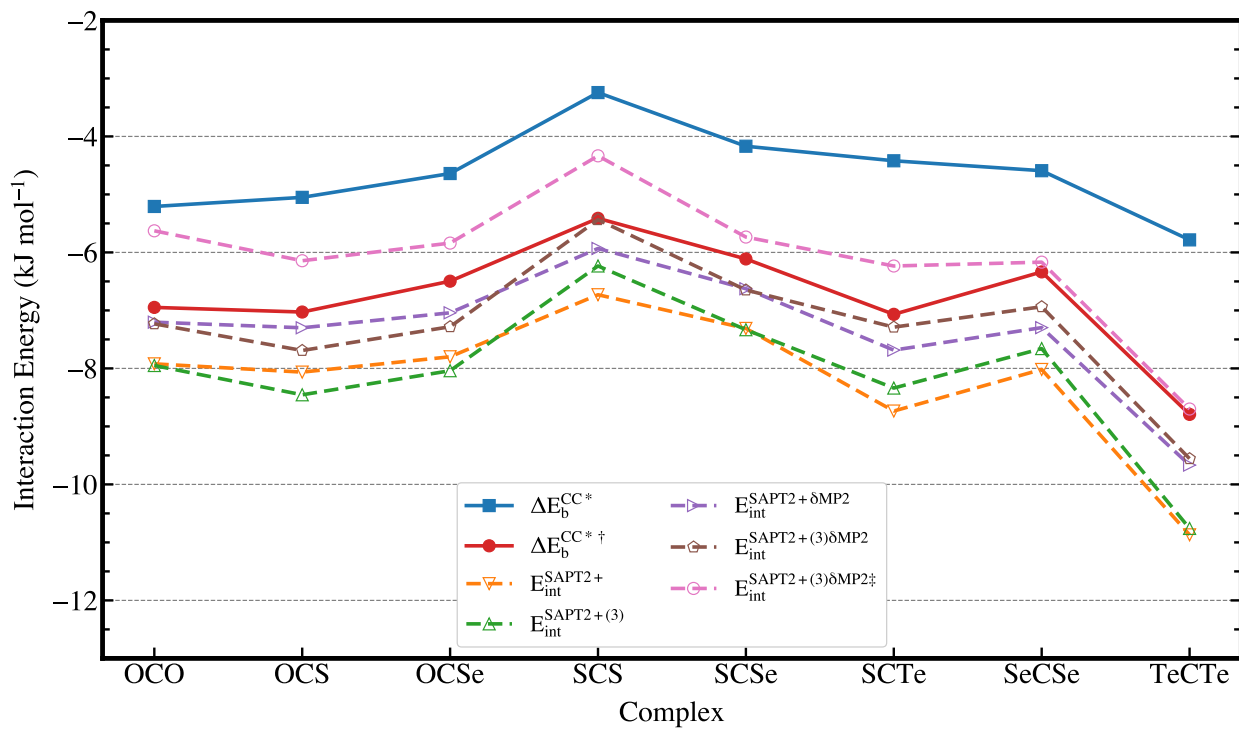


Figure S10: Comparison on interaction energies obtained from supermolecular at CCSD(T) level (solid lines, solid markers) and variants of SAPT approaches (dashed lines, empty markers).

We note in passing that better agreements between the supramolecular and SAPT approaches can be achieved by correcting the energy values from either approach. Also plotted in Figure S10 are results from the two methods proposed by Emamian *et. al.*,<sup>S4</sup> which accounts only half of the BSSE (referred to as  $\Delta E_b^{\text{CC}*\dagger}$ ), and Phan *et. al.*,<sup>S3</sup> which considers the ZPE correction for the SAPT's interaction energy ( $E_{\text{int}}^{\text{SAPT2+}(3)\delta\text{MP2}\ddagger}$ ). While both methods show enhanced alignments, the former results agree remarkably well with the best SAPT results. It should be cautious, though, that such an improvement does not implies the deviations from the two approaches are due to overcounting BSSE in the supramolecular approach.

## References

- (S1) Pracht, P.; Grimme, S.; Bannwarth, C.; Bohle, F.; Ehlert, S.; Feldmann, G.; Gorges, J.; Müller, M.; Neudecker, T.; Plett, C.; Spicher, S.; Steinbach, P.; Wesołowski, P. A.; Zeller, F. CREST—A program for the exploration of low-energy molecular chemical space. *The Journal of Chemical Physics* **2024**, *160*.
- (S2) Bannwarth, C.; Ehlert, S.; Grimme, S. GFN2-xTB—An Accurate and Broadly Parametrized Self-Consistent Tight-Binding Quantum Chemical Method with Multipole Electrostatics and Density-Dependent Dispersion Contributions. *Journal of Chemical Theory and Computation* **2019**, *15*, 1652–1671.
- (S3) Phan Dang, C.-T.; Tam, N. M.; Huynh, T.-N.; Trung, N. T. Revisiting conventional noncovalent interactions towards a complete understanding: from tetrel to pnicogen, chalcogen, and halogen bond. *RSC Advances* **2023**, *13*, 31507–31517.
- (S4) Emamian, S.; Lu, T.; Kruse, H.; Emamian, H. Exploring Nature and Predicting Strength of Hydrogen Bonds: A Correlation Analysis Between Atoms-in-Molecules Descriptors, Binding Energies, and Energy Components of Symmetry-Adapted Perturbation Theory. *Journal of Computational Chemistry* **2019**, *40*, 2868–2881.